Article

Not peer-reviewed version

# Graphene-Based PDLC Device Enabled by Water-Induced Interface Cleaning Process

Eun Mi Kim , Su Jin Kim , Go Bong Choi , Jaegeun Lee , Min Mo Koo , Jaewoong Kim , Young Won Kim , Jongho Lee , Jin Hyeok Kim * , Tae Hoon Seo *

Posted Date: 20 July 2023

doi: 10.20944/preprints202307.1434.v1

Keywords: Four layer graphene, Polymer dispersed liquid crystal, Smart window, Water induced interface cleaning, adhesion

*Article*

# Graphene-Based PDLC Device Enabled by Water-Induced Interface Cleaning Process

**Eun Mi Kim [1,5,†], Su-Jin Kim [1,5,†], Go Bong Choi [2], Jaegeun Lee [3], Min Mo Koo [4], Jaewoong Kim [4], Young Won Kim [1], Jongho Lee [1], Jin Hyeok Kim [5,6,*] and Tae Hoon Seo [1,*]**

[1] Green Energy and Nano Technology & R&D Group, Korea Institute of Industrial Technology (KITECH), Gwang-ju 61012, Republic of Korea, kimeunmi@kitech.re.kr (E.M.K.), ksjhy4@kitech.re.kr (S.-J.K.), ywkim@kitech.re.kr (Y.W.K.), jholee@kitech.re.kr (J.L.)

[2] Korea Advanced Institute of Science and Technology (KAIST), 291 Daehak-ro, Yuseong-gu, Daejeon, 34141, Republic of Korea, gbchoi@kaist.ac.kr

[3] School of Chemical Engineering, Pusan National University, Busan, 46261, Republic of Korea, jglee@pusan.ac.kr

[4] Automotive Materials & Components R&D Group, Korea Institute of Industrial Technology (KITECH), Gwangju 61012, Republic of Korea, mmkoo@kitech.re.kr (M.M.K.), kjw0607@kitech.re.kr (J.K.)

[5] School of Materials Science & Engineering, Chonnam National University, Gwang-ju 61186, Republic of Korea

[6] Optoelectronic Convergence Research Center, Department of Materials Science and Engineering, Chonnam National University, Gwang-ju 61186, Republic of Korea

* Correspondence: thseo@kitech.re.kr (T.H.S.), jinhyeok@jnu.ac.kr (J.H.K.)

† These authors contributed equally to this work.

**Abstract:** We report the use of four-layer graphene (4LG) as a highly reliable transparent conductive electrode (TCE) for polymer-dispersed liquid crystal (PDLC)-based smart window devices. The adhesion between 4LG and the substrate was successfully improved through a water-induced interface-cleaning (WIIC) process. We compared the performance of a device with a WIIC-processed 4LG electrode with that of devices with a conventional Indium tin oxide (ITO) electrode and a 4LG electrode without a WIIC. With the application of the WIIC process, the PDLC smart window with a 4LG electrode exhibited reduced turn-on voltage and haze compared to 4LG without the WIIC process and characteristics comparable to those of the ITO electrode. Based on our observations, we conclude that 4LG with WIIC is a promising TCE for flexible smart windows.

**Keywords:** four layer graphene; polymer dispersed liquid crystal; smart window; water induced interface cleaning; adhesion

## 1. Introduction

The concept of a "net-zero-energy building," which refers to the balance of emissions and energy in a building, attracts considerable attention and is considered a feasible solution instead of a distant future objective [1]. Several efforts have been made to reduce the energy consumed by building services such as ventilation, heating, and air conditioning [2,3]. Smart window technology is expected to play a crucial role in achieving eco-friendly energy savings in buildings because windows are among the most energy-efficient components. In particular, smart window devices based on polymer-dispersed liquid crystals (PDLC) offer various advantages, including a simple electrode-sandwiched design, straightforward fabrication process, quick response time, and durability [4–6]. Despite decades of steady and intensive research on liquid crystal (LC) coatings, polymer matrices, and ultraviolet aging, transparent conductive electrodes (TCE) continue to pose major challenges. TCE require low sheet resistance, high transparency, flexibility, and low cost. Indium tin oxide (ITO) has been commercially utilized as a TCE in PDLC-based smart windows, owing to its high optical transmittance and low sheet resistance. However, the ITO layer has several drawbacks such as rising prices due to the scarcity of indium, chemical instability towards acidic and basic sources, and high processing temperatures [7,8]. Furthermore, its application in flexible smart windows is severely

 doi:10.20944/preprints202307.1434.v1



hampered by its fragility when the substrate is bent or stretched by external force [9,10]. Therefore, alternative electrodes that can match or surpass ITO's optical and electrical properties of ITO, without any disadvantages, are required. Numerous alternative materials such as carbon nanotubes [11], graphene [12–15], conductive polymers [16,17], and metal nanowires [18,19] have been explored and developed to replace ITO layers. Graphene has recently emerged as a promising alternative owing to its outstanding optical and electrical properties and thermal and chemical stabilities. Furthermore, graphene exhibits the flexibility required for use in smart windows. Pioneering studies have demonstrated PDLC-based smart window devices that employ graphene layers as TCEs on glass and other flexible plastic substrates. However, the lack of adhesion between graphene and its substrate can lead to local delamination, folding, and bending when exposed to a weak external force, resulting in the mechanical failure of graphene-based devices at their interface [20–22]. In addition, graphene cannot outperform ITO as the TCE due to its high sheet resistance of approximately 1.0 KΩ/ [12–14]. Consequently, for commercialization, improving the interfacial adhesion between graphene and the substrates with low sheet resistance is necessary. In this study, we report a graphene-based PDLC device using a four-layer graphene (4LG) TCE with a water-induced interface cleaning (WIIC) process. 4LG is the optimal layer for balancing the sheet resistance and transmittance trade-offs. Unlike single-layer graphene, 4LG exhibits electrical characteristics comparable to those of ITO. The WIIC process is simple and highly effective for eliminating impurities and improving the adhesion between graphene and the substrate. We demonstrated that the performance and stability of our graphene-based PDLC device are comparable to those obtained using ITO electrodes as conducting layers.

## 2. Materials and Methods

### *2.1. Synthesis of graphene and transfer to glass substrate*

The graphene layers employed in this study were produced by thermal chemical vapor deposition (TCVD) on 70 m polycrystalline copper foils. $CH_4$ at 10 standard cubic centimeters per minute (sccm) and $H_2$ at 100 sccm were used as the precursors for graphene formation at 1020 °C for 18 min under a growth pressure of 0.13 Torr. Further details can be found in. 23. Following growth, graphene was transferred to a glass substrate at 110 °C using a thermal release tape. We obtained 4LG using a four-step transfer procedure.

### *2.2. Water-Induced Interface Cleaning (WIIC) process*

Figure 1a shows a schematic of the experimental design adopted in this study. We performed WIIC to improve the adhesion between graphene and the glass substrate. 4LG/glass was submerged in deionized water for 1 min. The 4LG/glass sample was then heated in a chamber at 200 °C under vacuum for 10 min using fast thermal processing equipment. Theoretically, because graphene has the smallest kinetic diameter [24–27], i.e., no gas molecules can pass through it. Water molecules that are entrapped between graphene and the substrate can only move in the lateral directions compared to the vertical ones, which would allow them to sweep impurities away. Consequently, the removal of impurities significantly improves the adhesion force. In the final stage, the sample was cooled to room temperature under an Ar flow of 500 sccm.

### *2.3. Fabrication of PDLC device*

To fabricate the PDLC devices, we prepared three different TCEs: (1) conventional Indium Tin Oxide (ITO), (2) 4LG without WIIC (w/o WIIC), and (3) 4LG with WIIC (w/WIIC). The PDLC, composed of a liquid crystal, prepolymer, and photoinitiator, was acquired from Qingdao QY Liquid Crystal Co., Ltd. (QYPDLC-100). To produce a uniform PDLC device thickness, 20 μm silica microspheres were used. The combined PDLC and microsphere spacer solution was dripped onto the bottom electrode of the glass substrate. Subsequently, a sample with the same electrode is placed on top to form a sandwich with a shift. Finally, the PDLC mixture was cured by exposing the device

Preprints (www.preprints.org) | NOT PEER-REVIEWED | Posted: 20 July 2023 doi:10.20944/preprints202307.1434.v1



to a UV lamp with an intensity of 1 mW/cm² at 365 nm for 60 s. Figure 1b shows a schematic of the fabricated PDLC device with 4LG as the TCE.

*2.4. Characterization*

Raman spectroscopy (Renishaw) was used to determine the number of layers and the quality of graphene, utilizing the 514 nm-line of an Ar-ion laser as an excitation source. Field-emission scanning electron microscopy was utilized to examine the surface morphology of graphene transferred to $SiO_2$/Si substrate (FESEM, NovaSEM 450). To confirm the uniformity and electrical properties, sheet resistance mapping measurements were performed using a non-contact sheet resistance meter and a Hall measurement system. Transmittance and haze were measured as functions of various driving voltages using a UV-Vis-NIR spectrophotometer (Lambda750, Perkin Elmer) and a haze meter (Nippon Denshoku, NDH5000), respectively.

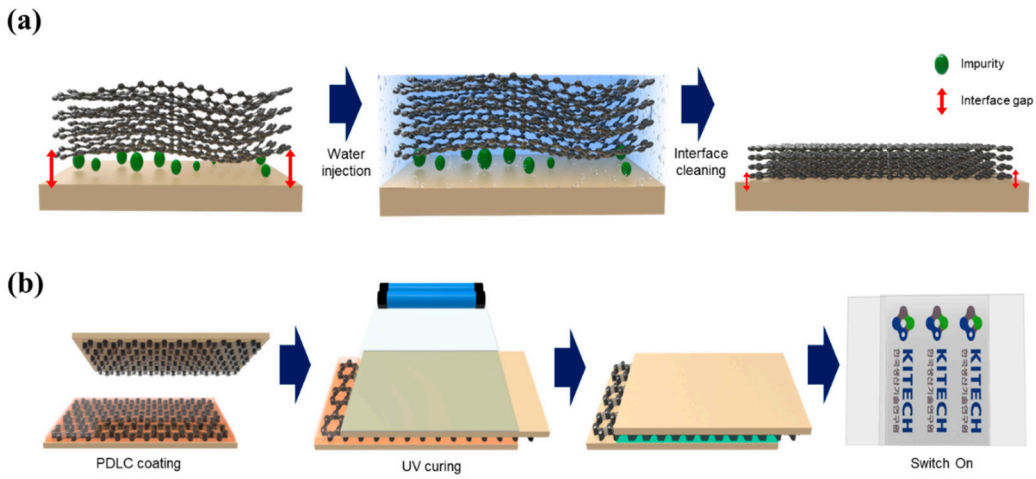


**Figure 1.** Schematic diagram of (a) WIIC process and (b) fabrication process of graphene-based PDLC device.

## 3. Results

*3.1. Number of graphene layer*

The two crucial considerations for the use of TCEs in PDLC devices are optical transmittance and sheet resistance, because these two parameters significantly impact the device's performance. Although the use of 1LG is desirable in terms of optical transmittance, it suffers from a high sheet resistance. Hence, we attempted to balance sheet resistance and transmittance by increasing the number of graphene layers. Based on our experience, we hypothesized that 4LG would be suitable as a TCE in PDLC devices, exhibiting both high transmittance and low sheet resistance. To test this hypothesis, we first confirmed the successful transfer of high-quality 1LG and 4LG onto substrates. We transferred 1LG and 4LG to $SiO_2$/Si substrates and acquired their Raman spectra to investigate their quality and quantity. Figure 2a shows the Raman spectra measured using the 514 nm-line of an Ar ion laser. The spectrum of 1LG shows two prominent peaks: the G band at 1594 $cm^{-1}$ and the 2D band at 2703 $cm^{-1}$. The Raman spectrum of 1LG exhibited typical monolayer graphene characteristics, particularly a very sharp Lorentzian peak with a full width at half maximum (FWHM) of 30 $cm^{-1}$, symmetric shape, and a 2D to G intensity ratio greater than two. The 2D peak broadens and becomes less intense as the number of graphene layers increases, whereas the G peak becomes more intense [28,29]. The spectra of 4LG had a lower 2D to G intensity ratio (0.79) and a larger FWHM (38 $cm^{-1}$) than those of 1LG. Moreover, the so-called defects-induced or disorder-induced D-band peak at 1350 $cm^{-1}$ is minuscule, indicating that 4LG is high quality with few defects. The transmittances and sheet resistances of the four TCEs are shown in Figure 2b. The transmittances of the conventional ITO, 1LG, and 4LG without the WIIC process, and 4LG with the WIIC process at 550 nm were 90.0%, 97.5%,

Preprints (www.preprints.org) | NOT PEER-REVIEWED | Posted: 20 July 2023 doi:10.20944/preprints202307.1434.v1



89.6%, and 89.8%, respectively. As expected, the 1LG TCE exhibits the highest transmittance. Nevertheless, the transmittance of the 4LG TCE is comparable to that of the ITO TCE. The sheet resistance was also determined. Sheet-resistance measurements were performed using a Hall measurement system. The obtained sheet resistance values of conventional ITO, 1LG, 4LG without WIIC, and 4LG with WIIC are 30±2 Ω/ , 202±10 Ω/ , 49±4 Ω/ , and 57±2 Ω/ , respectively. The sheet resistance of 4LG with the WIIC process was slightly higher than that of 4LG without the WIIC process. This can be attributed to the fact that some defects in 4LG are linked to oxygen groups during the WIIC process. Overall, the 4LG TCEs simultaneously exhibited high transmittance and low sheet resistance, which is consistent with our hypothesis.

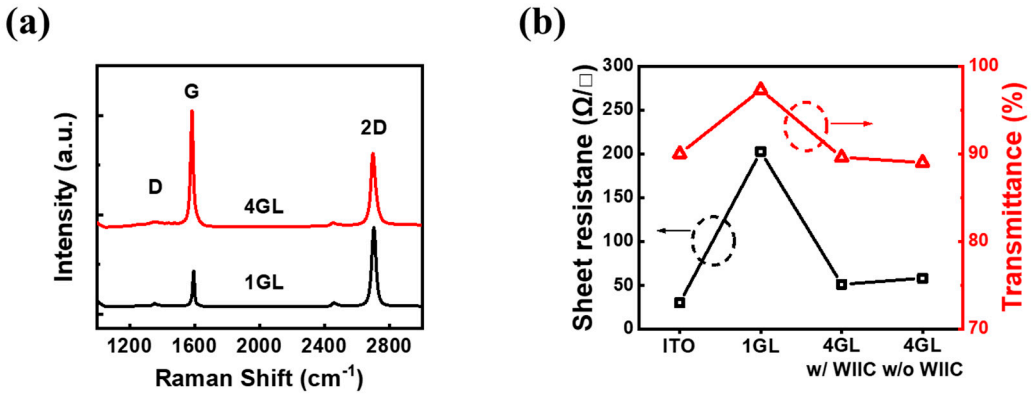


**Figure 2.** (a) Raman spectra of 1LG and 4LG transferred to a $SiO_2$/Si substrate. (b) transmittance and sheet resistance of ITO, 1LG, 4LG with WIIC, and 4LG without WIIC, respectively.

*3.2. Effect of WIIC*

Our second strategy to improve the performance of graphene-based PDLC devices was to employ the WIIC process to remove impurities at the interface between the TCE and substrate. We propose that the WIIC process offers two advantages. First, the TCE was uniform throughout the study area. Second, it improved the adhesion between the TCE and the substrate. Uniformity was already revealed when the sheet resistance was measured. The sheet resistance of 4LG without and 4LG with WIIC were 49±4 Ω/ and 57±2 Ω/, respectively. The standard deviation of the sheet resistance of 4LG with WIIC was half that of 4LG without WIIC. To confirm the uniformity of 4LG o on a large scale, we performed 4-point mapping for a 200 mm × 200 mm area of 4LG with and without WIIC, as depicted in Figure 3a,b. A sheet resistance value of 58±2 Ω/sq is observed for the 4LG with WIIC process, which is slightly higher than the value of 51±5 Ω/sq obtained for 4LG without WIIC process. This result is consistent with the Hall measurements. Although the sheet resistance increased because of the WIIC procedure, the entire area had a uniform sheet resistance value. The elimination of impurities, as indicated by the white circle in Figure 3a, may be responsible for this. The effect of the WIIC process is further supported by the on/off optical images shown in Figure 4a,b. The optical image of the PLDC device with a 4LG electrode without the WIIC process at an applied voltage is unclear and shows the graphene-burning phenomenon resulting from the high power consumption of graphene [30,31], as marked by the blue circle in Figure 4a. Because of the current crowding induced by impurities and adhesion between the graphene and the substrate at 60 V injection, an excessive quantity of power builds up under the graphene electrode in the device, destroying the graphene with Joule heat. As illustrated in Figure 4b, in the case of the 4LG electrode following the application of the WIIC process, the device in the ON state was nearly transparent and uniform across the entire operation region. This clearly indicates that the 4LG electrode with the WIIC process as a transparent conductive layer can act as an efficient lateral current diffusion channel. The WIIC process effect can be evaluated using the above results obtained from the PDLC device, but the adhesion between the 4LG electrode and the substrate could not be verified. To confirm whether the WIIC process was capable of enhancing the adherence of the 4LG electrode to the substrate, we fabricated patterned graphene using photolithography and etching over a large area of 200 mm × 200

Preprints (www.preprints.org) | NOT PEER-REVIEWED | Posted: 20 July 2023 doi:10.20944/preprints202307.1434.v1



mm, as shown in Figure 5a. To form patterned graphene, the CVD-grown graphene films were transferred four times onto a glass substrate. Thereafter, the patterned region was covered with a protective photoresist (PR) as an etchant mask and graphene was patterned using an inductively coupled plasma reactive-ion etcher with $O_2$ plasma. Finally, the PR was removed using acetone. Figure 5b and c show the optical images of the patterned graphene without and with the WIIC process, respectively. The surface of patterned graphene without a WIIC process is readily and partially peeled-off during fabrication owing to the lack of chemical reactivity of graphene, which consists of the C-C bond of $sp^2$ hexagonally arranged carbon atoms with no dangling bonds [20–22,32]. When the WIIC process was applied, we observed a cleanly patterned graphene surface without peeling. This is as a result of the fact that the adhesion of graphene to the substrate was stronger than its attachment to the PR, which is indicative of enhanced adhesion.

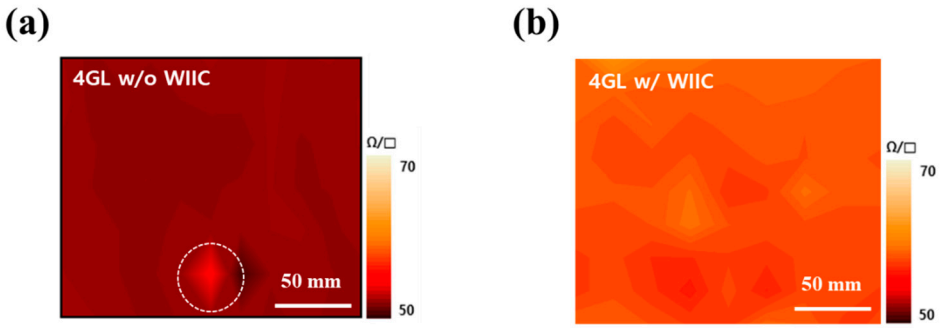


**Figure 3.** 4-point mapping images of (a) 4LG without WIIC process and (b) 4LG with WIIC process at a 200 mm × 200 mm area.

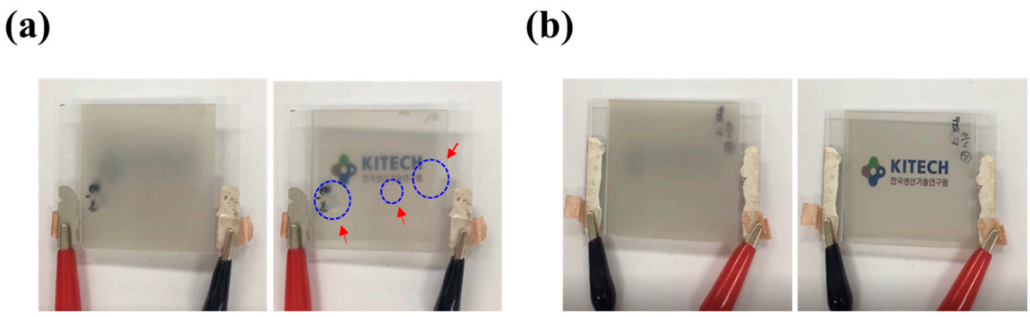


**Figure 4.** Optical images for PDLC devices of (a) 4LG without WIIC process and (b) 4LG with WIIC process in on/off state.

Preprints (www.preprints.org) | NOT PEER-REVIEWED | Posted: 20 July 2023 doi:10.20944/preprints202307.1434.v1



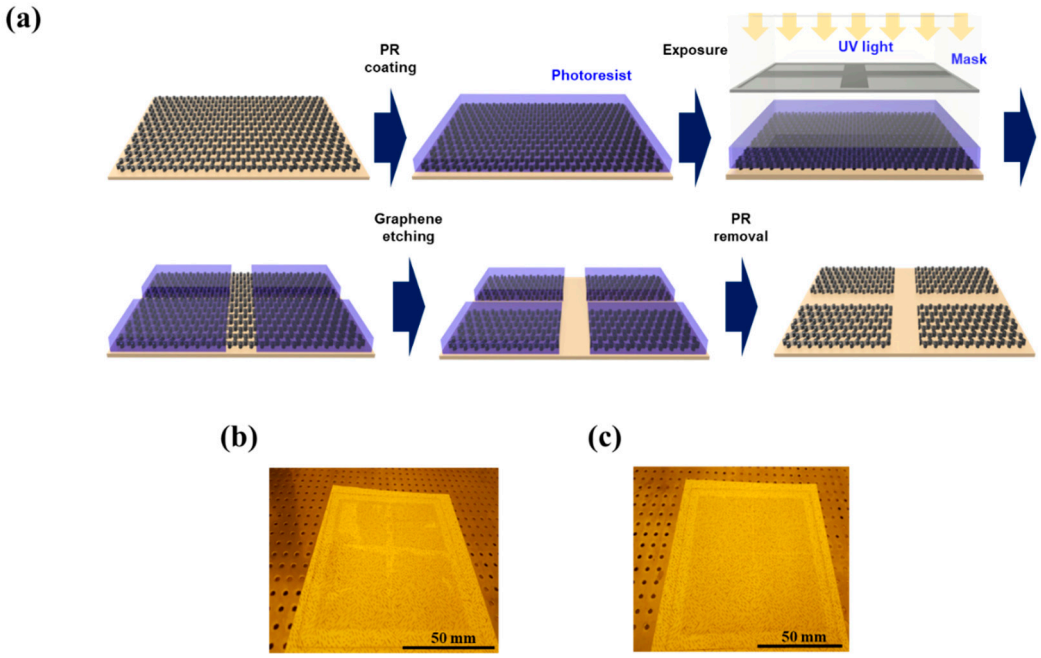


**Figure 5.** (a) Schematic diagram of fabrication process for the patterned 4LG using photolithography and etching. Optical images of the patterned 4LG (b) without WIIC process and (c) with WIIC process.

*3.3. Performance of PDLC device*

The properties of the PDLC device were examined to understand the potential of the WIIC process. Figures 6a,b show the transmittance at 550 nm and haze of the PDLC devices with conventional ITO, 4LG without the WIIC process, and 4LG with the WIIC process, respectively, as a function of the applied voltage. All devices scattered or reflected almost all the incident light when turned off. As the applied voltage increased, more incident light was transmitted through the device, reaching a saturation state at a critical voltage. As shown in Figure 6a, the transmittance of the device with the conventional ITO electrode rapidly increased at injection voltages exceeding 15 V and reached a maximum transmittance of 68% at 60 V. For the bare 4LG electrode, the transmittance increased at driving voltages above 35 V and reached a maximum transmittance of 48% at 60 V. The relatively high turn-on voltage and low transmittance associated with the bare graphene electrode were due to insufficient current spreading due to poor contact between graphene and the substrate. When the WIIC process was applied to the bare 4LG electrode, the transmittance-voltage curves revealed a considerable reduction in the turn-on voltage of 17 V and an increase in the maximum transmittance of 20% compared to those of the 4LG electrode-based device without the WIIC process. This is attributed to the improvement in the adhesion level between the graphene layer and substrate, which indicates that the 4LG electrode with the WIIC process serves as the current-spreading electrode of the PDLC device. The haze as a function of the injection voltage for the PDLC devices with the three different TCEs, as shown in Figure 6a, is illustrated in Figure 6b. The haze values of ITO, 4LG without WIIC, and 4LG with WIIC at 60 V were measured to be 5, 22, and 10%, respectively. By applying the WIIC process, the haze was significantly reduced by approximately 12% compared with that of the 4LG electrode without the WIIC process. As shown in Figure 6a,b, even if the sheet resistance increased after utilizing the WIIC process, this was due to the improved interfacial adhesion. However, the haze and turn-on voltages for the PDLC device with the 4LG electrode and the WIIC process were still slightly higher than those of the PDLC device with the conventional ITO electrode owing to the relatively high sheet resistance. If the optoelectrical performance of graphene is further improved by optimizing the graphene transfer and improving the electrical properties of the graphene layer in the CVD synthesis, it will be suitable for use as a TCE in flexible devices owing to the lack of flexibility in ITO. Figure 6c illustrates the temporal characteristics of all the PDLC

Preprints (www.preprints.org) | NOT PEER-REVIEWED | Posted: 20 July 2023 doi:10.20944/preprints202307.1434.v1



devices. During the off-to-on and on-to-off voltage transitions, the rise and decay times were defined as the times required for the transmittance to increase from 10% to 90%, respectively. Rise times of ITO, 4LG without WIIC, and 4LG with WIIC were 1.1, 1.4, and 1.6 ms, respectively, and their decay times 41, 27, and 29 ms, respectively. The rise time of 4LG with WIIC was shorter than that of 4LG without WIIC owing to the reduced sheet resistance. While all other material properties are constant, it is widely known that the decay time increases with the droplet size. We believe that the decrease in the decay time of PDLC devices with graphene electrodes results of smaller LC droplets in the polymer matrix [14]. Details of the decay time results will be discussed in future studies.

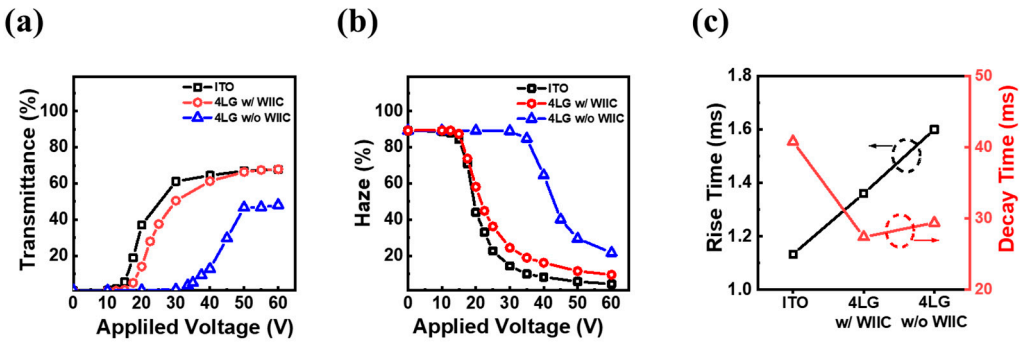


**Figure 6.** (a) Transmittance (@ 550 nm) and (b) haze according to applied voltage in PDLC devices of ITO, 4LG with WIIC process, and 4LG without WIIC process, respectively. (c) Rise and decay time for PDLC devices of three different TCEs investigated in this work.

## 4. Conclusions

We investigated the effect of adhesion on the performance of 4LG as a TCEs in PDLC devices. WIIC effectively increased the adhesion between 4LG and the substrate. The sheet resistance of 4LG with WIIC process used in this work is 58±2 Ω/ . Furthermore, it exhibited a uniform sheet resistance over the entire area. A PDLC device with the 4LG and WIIC processes was fabricated to confirm the WIIC effect. The device with the WIIC process offered a 17 V reduction in turn-on voltage, 20% improvement in maximum transmittance, and 12% reduction in haze compared to the device without the WIIC process. Our findings suggest that graphene with increased adhesion and ultralow resistance as a TCE has considerable potential for use in flexible devices owing to its stability.

**Author Contributions:** Conceptualization, E.M.K. and T.H.S.; investigation, E.M.K., S.-J.K. and M.M.K.; data curation, E.M.K., G.B.C., J.K., Y.W.K. and T.H.S.; experiments, E.M.K. and S.-J.K.; formal analysis, E.M.K. and S.-J.K., writing-original draft, E.M.K.; visualization, G.B.C., validation, J.L. and J.H.K.; writing, J.L. and T.H.S.; review, J.L. and T.H.S.; editing, J.L. and T.H.S.; methodology, J.L. and J.H.K.; supervision, J.H.K. and T.H.S. All authors have read and agreed to the published version of the manuscript.

**Funding:** This study was conducted with the support of the Korea Institute of Industrial Technology under the Development of Core Technologies for Smart Mobility (KITECH JA-23-0011)". This work was supported by the Basic Science Research Program through the National Research Foundation of Korea (NRF), funded by the Ministry of Education, Science, and Technology (NRF-2022R1F1A1074422) and by the Korea Institute of Marine Science and Technology Promotion (KIMST), funded by the Ministry of Oceans and Fisheries, Korea (20200599).

**Data Availability Statement:** The data presented in this study are available on request from the corresponding author.

**Conflicts of Interest:** The authors declare no conflict of interest.

## References

1. Marszal, A.J.; Heiselberg, P.; Bourrelle, J.S.; Musall, E.; Voss, K.; Sartori, I.; Napolitano, A. Zero Energy Building – A review of definitions and calculation methodologies. *Energy Build.* **2011**, *43*, 971–979. https://doi.org/10.1016/j.enbuild.2010.12.022.

2. Ke, Y.; Zhou, C.; Zhou, Y.; Wang, S.; Chan, S.H.; Long Y. Emerging Thermal-Responsive Materials and Integrated Techniques Targeting the Energy-Efficient Smart Window Application. Adv. Funct. Mater. 2018, 28, 1800113. https://doi.org/10.1002/adfm.201800113.
3. Baetens, R.; Jelle, B.P.; Gustavsen, A. Properties, requirements and possibilities of smart windows for dynamic daylight and solar energy control in buildings: A state-of-the-art review. *Sol. Energy Mater. Sol. Cells.* **2010**, *94*, 87–105. https://doi.org/10.1016/j.solmat.2009.08.021.
4. Jung, D.; Choi, W.; Park, J.Y.; Kim, K.B.; Lee, N.; Seo, Y.; Kim, H.S.; Kong, N.K. Inorganic gel and liquid crystal based smart window using silica sol-gel process. *Sol. Energy Mater. Sol. Cells.* **2017**, *159*, 488–495. https://doi.org/10.1016/j.solmat.2016.10.001.
5. Park, J.Y.; Kim, H.K. Highly stretchable polymer-dispersed liquid crystal-based smart windows with transparent and stretchable hybrid electrodes. *RSC Adv.* **2018**, *8*, 36549–36557. https://doi.org/10.1039/c8ra07033d.
6. Huang, J.; Li, J.; Xu, J.; Wang, Z.; Sheng, W.; Li, H.; Yang, Y.; Song, W. Simultaneous achievement of high visible transmission and near-infrared heat shielding in flexible liquid crystal-based smart windows via electrode design. *Sol. Energy.* **2019**, *188*, 857–864. https://doi.org/10.1016/j.solener.2019.06.063.
7. Na, S.I.; Kim, S.S.; Jo, J.; Kim, D.Y. Efficient and Flexible ITO-Free Organic Solar Cells Using Highly Conductive Polymer Anodes. *Adv. Mater.* **2008**, *20*, 4061–4067. https://doi.org/10.1002/adma.200800338.
8. Wang, X.; Zhi, L.; Müllen, K. Transparent, conductive graphene electrodes for dye-sensitized solar cells. *Nano Lett.* **2008**, *8*, 323–327. https://doi.org/10.1021/nl072838r.
9. Kumar, A.; Zhou, C. The race to replace tin-doped indium oxide: which material will win?. *ACS Nano.* **2010**, *4*, 11–14. https://doi.org/10.1021/nn901903b.
10. Wu, H.; Kong, D.; Ruan, Z.; Hsu, P.C.; Wang, S.; Yu, Z.; Carney, T.J.; Hu, L.; Fan, S.; Cui, Y. A transparent electrode based on a metal nanotrough network. *Nat. Nanotechnol.* **2013**, *8*, 421–425. https://doi.org/10.1038/nnano.2013.84.
11. Chen, Z.; Chen, X.D.; Wang, H.; Li, X.; Lin, L.; Chen, K.; Ci, H.; Wu, X.; Zhang, Y.; Liu, Z. One-Step Growth of Graphene/Carbon Nanotube Hybrid Films on Soda-Lime Glass for Transparent Conducting Applications. *Adv. Electron. Mater.* **2017**, *3*, 1700212. https://doi.org/10.1002/aelm.201700212.
12. Kim, Y.; Kim, K.; Kim, K.B.; Park, J.Y.; Lee, N.; Seo, Y. Flexible polymer dispersed liquid crystal film with graphene transparent electrodes. *Curr. Appl. Phys.* **2016**, *16*, 409–414. https://doi.org/10.1016/j.cap.2016.01.003.
13. Liu, F.; Wang, G.; Pal, K.; Zhan, B.; Liu, S.; Wen, D.; Ye, S. Flexible Polymer Dispersed Liquid Crystal Module with Graphene Electrode. *J. Nanosci. Nanotechnol.* **2015**, *15*, 9829–9833. https://doi.org/10.1166/jnn.2015.11706.
14. Chung, S.H.; Noh, H.Y. Polymer-dispersed liquid crystal devices with graphene electrodes. Opt. Express. **2015**, *23*, 32149–32157. https://doi.org/10.1364/OE.23.032149.
15. Marinova, V.; Petrov, S.; Napoleonov, B.; Mickovski, J.; Petrova, D.; Dimitrov, D.; Hsu, K.Y.; Lin, S.H. Multilayer Graphene for Flexible Optoelectronic Devices. *Mater. Proc.* **2021**, *65(4)*, 1–6. https://doi.org/10.3390/IOCN2020-07900.
16. Kim, Y.B.; Park, S.; Hong, J.W. Fabrication of flexible polymer dispersed liquid crystal films using conducting polymer thin films as the driving electrodes. *Thin Solid Films.* **2009**, *517*, 3066–3069. https://doi.org/10.1016/j.tsf.2008.11.112.
17. Wang, P.C.; MacDiarmid, A.G. Integration of polymer-dispersed liquid crystal composites with conducting polymer thin films toward the fabrication of flexible display devices. *Displays.* **2007**, *28*, 101–104. https://doi.org/10.1016/j.displa.2007.04.006.
18. Khaligh, H.H.; Liew, K.; Han, Y.; Abukhdeir, N.M.; Goldthorpe, I.A. Silver nanowire transparent electrodes for liquid crystal-based smart windows. *Sol. Energy Mater. Sol. Cells.* **2015**, *132*, 337–341. https://doi.org/10.1016/j.solmat.2014.09.006.
19. Kim, D.J.; Hwang, D.Y.; Park, J.Y.; Kim, H.K. Liquid crystal–Based flexible smart windows on roll-to-roll slot die–Coated Ag nanowire network films. *J. Alloys Compd.* **2018**, *765*, 1090–1098. https://doi.org/10.1016/j.jallcom.2018.06.285.
20. Jiang, T.; Zhu, Y. Measuring graphene adhesion using atomic force microscopy with a microsphere tip. *Nanoscale.* **2015**, *7*, 10760–10766. https://doi.org/10.1039/c5nr02480c.
21. Cho, D.H.; Wang, L.; Kim, J.S.; Lee, G.H.; Kim, E.S.; Lee, S.; Lee, S.Y.; Hone, J.; Lee, C. Effect of surface morphology on friction of graphene on various substrates. *Nanoscale.* **2013**, *5*, 3063–3069. https://doi.org/10.1039/c3nr34181j.
22. Hammad, M.; Adjizian, J.J.; Sacré, C.H.; Huet, B.; Charlier, J.C.; Raskin, J.P.; Pardoen, T. Adhesionless and near-ideal contact behavior of graphene on Cu thin film. *Carbon.* **2017**, *122*, 446–450. https://doi.org/10.1016/j.carbon.2017.06.037.
23. Seo, T.H.; Lee, S.; Cho, H.; Chandramohan, S.; Suh, E.K.; Lee, H.S.; Bae, S.K.; Kim, S.M.; Park, M.; Lee. J.K.; Kim, M.J. Tailored CVD graphene coating as a transparent and flexible gas barrier. *Sci. Rep.* **2016**, 6, 24143. https://doi.org/10.1038/srep24143.

24. Leenaerts, O.; Partoens, B.; Peeters, F.M. Graphene: A perfect nanoballoon. *Appl. Phys. Lett.* **2008**, *93*, 193107. https://doi.org/10.1063/1.3021413.
25. Bunch, J.S.; Verbridge, S.S.; Alden, J.S.; van der Zande, A.M.; Parpia, J.M.; Craighead, H.G.; McEuen, P.L. Impermeable atomic membranes from graphene sheets. *Nano Lett.* **2008**, *8*, 2458–2462. https://doi.org/10.1021/nl801457b.
26. Karpan, V.M.; Giovannetti, G.; Khomyakov, P.A.; Talanana, M.; Starikov, A.A.; Zwierzycki, M.; van den Brink, J.; Brocks, G.; Kelly, P.J. Graphite and graphene as perfect spin filters. *Phys. Rev. Lett.* **2007**, *99*, 176602. https://doi.org/10.1103/PhysRevLett.99.176602.
27. Gadipelli, S.; Guo, Z.X. Graphene-based materials: Synthesis and gas sorption, storage and separation. *Prog. Mater. Sci.* **2015**, *69*, 1–60. https://doi.org/10.1016/j.pmatsci.2014.10.004.
28. Wang, T.Y.; Ni, Zh.; Yu, T.; Shen, Z.X.; Wang, H.M.; Wu, Y.H.; Chen, W.; Wee, A.T.S. Raman Studies of Monolayer Graphene: The Substrate Effect. *J. Phys. Chem. C.* **2008**, *112*, 10637–10640. https://doi.org/10.1021/jp8008404.
29. Graf, D.; Molitor, F.; Ensslin, K.; Stampfer, C.; Jungen, A.; Hierold, C.; Wirtz, L. Spatially resolved Raman spectroscopy of single- and few-layer graphene. *Nano Lett.* **2007**, *7*, 238–242. https://doi.org/10.1021/nl061702a.
30. Kim, B.J.; Lee, C.M.; Jung, Y.H.; Baik, K.H.; Mastro, M.A.; Hite, J.K.; Eddy, C.R.; Kim, J.H. Large-area transparent conductive few-layer graphene electrode in GaN-based ultra-violet light-emitting diodes. *Appl. Phys. Lett.* **2011**, *99*, 143101. https://doi.org/10.1063/1.3644496.
31. Seo, T.H.; Kim, B.K.; Shin, G.U.; Lee, C.H.; Kim, M.J.; Kim, H.; Suh, E.K. Graphene-silver nanowire hybrid structure as a transparent and current spreading electrode in ultraviolet light emitting diodes. *Appl. Phys. Lett.* **2013**, *103*, 051105. https://doi.org/10.1063/1.4817256.
32. Kim, Y.J.; Seo, T.H.; Kim, Y.H.; Suh, E.K.; Bae, S.K.; Hwang, J.Y.; Kim, J.W.; Kang, Y.J.; Kim, M.J.; Ahn, S.H. Two-Dimensional Stacked Composites of Self-Assembled Alkane Layers and Graphene for Transparent Gas Barrier Films with Low Permeability. Nano. lett. **2022**, *22*, 286–293. https://doi.org/10.1021/acs.nanolett.1c03761.